Eur. Phys. J. Special Topics **223**, 347–361 (2014)

DOI: 10.1140/epjst/e2014-02095-0

THE EUROPEAN PHYSICAL JOURNAL SPECIAL TOPICS

Regular Article

Computer simulation of heterogeneous nucleation of colloidal crystals at planar walls

B.J. Block[1], D. Deb[1,2], F. Schmitz[1], A. Statt[1], A. Tröster[1,3], A. Winkler[1], T. Zykova-Timan[1,4], P. Virnau[1], and K. Binder[1]

[1] Institut für Physik, Johannes Gutenberg-Universität, 55099 Mainz, Germany
[2] Chemistry Dept. University of Pittsburg, Pittsburg, PA 15261, USA
[3] Vienna University of Technology, Wiedner Hauptstr. 8-10/136, 1040 Vienna, Austria
[4] Department of Chemistry, University of Cambrige, CB2 1 EW, UK

Received 13 December 2013 / Received in final form 10 January 2014
Published online 28 February 2014

Abstract. A mini-review of the classical theory of heterogeneous nucleation at planar walls is given, and tests by Monte Carlo simulations for simple models of colloidal suspensions exhibiting a fluid-solid transition are described. This theory (due to Turnbull) assumes sphere-cap-shaped "sessile" droplets at the substrate, and the nucleation barrier that appears in the classical theory of homogeneous nucleation then is reduced by a factor depending on the Young contact angle. Various approximations inherent in this theory are examined: curvature corrections to the interfacial free energy of small droplets; neglect of anisotropy of the surface tension between crystal and fluid; neglect of corrections due to the line tension of the three-phase contact line; continuum rather than atomistic description. Also the problem of precise identification of the particles belonging (or not) to the "droplet" is discussed, and an alternative concept of extracting droplet properties from an analysis of finite size effects on phase coexistence in finite simulation boxes is explored. While the focus of our treatment is on the Asakura-Oosawa model of colloid polymer mixtures, also simple Ising/lattice gas models are considered to test some of these questions.

1 Introduction

Homogeneous nucleation considers the spontaneous formation of a (nanoscopic) domain of a new phase, that will be stable under the considered thermodynamic conditions, due to statistical fluctuations occurring in a metastable phase [1–3]. Under many conditions, the free energy barrier that needs to be overcome in such a (rare!) nucleation event is of the order of $50\,k_BT$ (k_B = Boltzmann's constant, T = absolute temperature), even if the nucleus contains only of the order of 100 particles. Thus experimentally "heterogeneous nucleation" where heterogeneities in the system lead to lower free energy barriers often is more relevant than homogeneous nucleation. Such heterogeneities may be ions or dust particles, when one considers nucleation of ice crystals in the atmosphere, or simply the walls of a

container when one considers solidification of a metallic melt, or nucleation at grain boundaries or dislocations in nucleation processes from metastable solid phases.

In the present paper we wish to consider only the idealized but generic case of nucleation of a crystal from a fluid phase at a perfectly flat and structureless planar wall, assuming conditions of incomplete wetting [4,5]. We focus on colloidal crystals for several reasons: (i) Due to the large size of colloidal particles, the corrugation of the substrate surface (on the atomistic scale) can be safely neglected, unlike the case of nucleation of crystals formed from atoms, where the possible misfit of the lattice periodicity of the crystal and the substrate needs to be taken into account. (ii) Crystal-fluid interfaces in colloidal systems can be observed experimentally by confocal microscopy with resolution on the single particle level [6]. (iii) Interactions among colloidal particles are tunable to a large extent (see e.g. [7]). As an example, here we shall focus on colloid-polymer mixtures [8–10] which can be described by the simple Asakura-Oosawa (AO) model [11–13] or its variants (e.g. [14]). The colloidal particles in the AO model are just described as hard spheres of diameter σ_c, and the polymers as soft spheres of diameter σ_p. While colloid-colloid and colloid-polymer overlap is strictly forbidden, polymer coils in good solvents can interpenetrate each other with little [14] energy cost (this energy cost is completely neglected in the AO model [11–13] so polymers behave like ideal gas particles). The presence of the polymers causes an entropic depletion attraction among the colloids. The range of this attraction is simply σ_p, and the strength is controlled by the concentration of the polymers (or their fugacity, respectively). If no polymers are present, the archetypical case of the simple hard sphere fluid emerges as a special case. While hard sphere fluids are a popular model for the study of homogeneous nucleation (see e.g. [16–18]), extensions of these studies to heterogeneous crystal nucleation at hard walls (e.g. [19–21]) are problematic, since there is evidence for complete wetting [22] of face-centered cubic crystals when close-packed planes are stacked at planar walls at the coexistence pressure of liquid-solid coexistence. If such a complete wetting occurs, one expects that crystal growth triggered by the wall should be possible without the need to overcome a nucleation barrier. Therefore, as will be shown in the present mini-review, use of the AO model is advantageous, because due to larger values of the liquid-solid surface tension it is easier to establish a situation of incomplete wetting [23,24].

We also note that for the gas-liquid type phase transition that occurs in the AO model for large enough values of the ratio $q = \sigma_p/\sigma_c$ ($q > 0.25$) variation of the range of a soft repulsive wall potential allows a convenient control of the contact angle θ of colloid rich droplets, from $\theta = 0$ (complete wetting) to $\theta = \pi$ (complete drying) [25,26]. It has been suggested [27] that tunable repulsive interactions between colloidal particles and walls could be created by coating the latter with a layer of grafted polymers (a "polymer brush" [28,29]); varying the grafting density and the molecular weight of the grafted polymers one can control the brush height [28,29] and hence the range and strength of the repulsion. As is well-known, this mechanism is also used for the stabilization of colloidal dispersions [30]. Thus, we emphasize that the topic that is reviewed here is relevant for possible experiments on colloid-polymer mixtures (though the experiments on nucleation phenomena in colloidal systems so far have focused on systems that can be approximately modeled as simple hard sphere systems [31–33]).

The outline of this mini-review is as follows: in Sect. 2, we summarize the main statements of the classical theory of homogeneous [1–3] and heterogeneous [34–37] nucleation, with an emphasis on the inherent assumptions and their possible limitations. In Sect. 3, we describe the model that is studied and in Sect. 4 we describe briefly how the relevant interfacial and wall excess free energies can be estimated. Section 5 reviews a simulation of wall-attached crystalline droplets [24], which are

studied both by a "thermodynamic" method (that previously had been validated for the Ising/lattice gas model [38,39]) and by a "microscopic" identification of the crystalline droplet in terms of local order parameters distinguishing particles belonging to the fluid from those belonging to the crystal [40–42].

Section 6 then discusses possible shortcomings of the approach that still may need to be investigated in the future, namely (i) curvature corrections to the interfacial free energy of a droplet, (ii) corrections due to the anisotropy of the crystal-liquid interfacial free energy and resulting nontrivial shape of the "droplet", and (iii) effects due to the excess free energy of the three-phase contact line ("line tension" [43–48]) where the crystal-fluid interface meets the wall. Section 7 then briefly summarizes our conclusions.

2 Classical theory of homogeneous and heterogeneous nucleation

The classical theory of nucleation addresses the limit where nucleation can be described as a steady state process, where a system in a metastable state slowly transforms by formation of nuclei of the new phase, at a "nucleation rate" given by an Arrhenius formula

$$J = \omega \exp[-\Delta F^*/k_B T]. \tag{1}$$

The prefactor ω contains kinetic factors (rates at which single particles are incorporated into a nucleus, etc.) [1–3,49], while the free energy barrier ΔF^* that needs to be overcome in a nucleation process, for homogeneous nucleation is traditionally described in terms of a competition between a bulk term, proportional to the volume V of the nucleus ($V = 4\pi R^3/3$ when one assumes the nucleus to be spherical) and a surface term proportional to the surface area A ($=4\pi R^2$). Then the formation free energy $\Delta F(R)$ is written as

$$\Delta F(R) = \Delta p V + \gamma A = -\Delta\mu(\rho_c - \rho_\ell)\left(\frac{4\pi R^3}{3}\right) + \gamma 4\pi R^2, \tag{2}$$

where γ is the interfacial tension between the nucleus and the surrounding fluid phase. According to the standard "capillarity approximation" [1–3,49] γ simply is taken as the surface tension associated with an (infinite) planar interface between the bulk coexisting phases (which have the densities ρ_c (crystal), ρ_ℓ (liquid), and must have zero chemical potential difference, $\Delta\mu = 0$). The bulk term ΔpV describes the gain in thermodynamic potential of the stable phase relative to the metastable phase, and is linearly expanded in $\Delta\mu$ at phase coexistence in Eq. (2). Minimizing $\partial(\Delta F(R))/\partial R = 0$ yields the critical radius R^* and the free energy barrier ΔF^*_{hom} against homogeneous nucleation,

$$R^* = \frac{2\gamma}{\Delta\mu(\rho_c - \rho_\ell)}, \quad \Delta F^*_{hom} = \frac{4\pi}{3} R^{*2}\gamma. \tag{3}$$

Obviously, Eq. (3) relies on the assumption that macroscopic descriptions in terms of bulk and interfacial free energy densities still can apply to nanoscopic droplets (which for physically relevant barriers may contain only of the order of 10^2 to 10^3 particles); both a possible dependence of γ on the radius R of the nucleus [50–68] and a deviation of nucleus shape from spherical due to the anisotropy of γ are neglected; and it is also neglected that steady state nucleation [49] is an idealization: it takes a time lag τ_ℓ after the quench (by which the system is brought from an equilibrium state into the metastable state with a supersaturation $S = \rho/\rho_\ell - 1 > 0$) to reach the "metastable equilibrium"; however, "metastable equilibrium" is an idealization,

since nucleation and growth leads to a (slow) decay of the metastable state, so $\Delta\mu$ is not strictly constant but slowly decaying with time, and finally the volume fraction of the system that still belongs to the metastable state shrinks [49] and ultimately vanishes. But a full treatment of this transient kinetics is very difficult (e.g., hydrodynamic interactions between particles in a colloidal dispersion have been shown to play a significant role [69,70]) and shall not be considered here further.

We now consider the extension of Eq. (3) to heterogeneous nucleation at a planar wall, assuming partial wetting of the crystal at fluid-solid coexistence, so $\Delta\gamma = \gamma_{wf} - \gamma_{ws} < \gamma$. If again the dependence of γ on the orientation of the interface (relative to the crystal axes) is neglected, one can use Young's equation for the contact angle [4,44,71]

$$\gamma \cos\theta = \Delta\gamma \tag{4}$$

and then the shape of the critical nucleus is simply a sphere cap [34,35], the sphere radius still being given by R^* [Eq. (2)], but the barrier ΔF^*_{het} is reduced by a factor $f(\theta)$, namely [34,35]

$$\Delta F^*_{het} = \Delta F^*_{hom} f(\theta), \quad f(\theta) = (1-\cos\theta)^2(2+\cos\theta)/4. \tag{5}$$

Obviously, such a continuum description of a crystalline nucleus containing of the order of 10^2 to 10^3 particles is questionable: For a face-centered cubic crystal, we expect an ABCABC-type stacking of close-packed planes parallel to the wall, and it is not at all obvious, that the surface of the nucleus is well approximated by a sphere cap; in fact, also the assumption of a facetted crystal surface could be made [71–73]. In addition, a correction due to the three-phase contact line must be expected [74–76] and this expectation is in agreement with simulations of wall-attached droplets in the lattice gas model [38,39]. Thus, it is a nontrivial question whether Eqs. (4), (5) are useful for crystal nucleation at substrates.

In the following chapters we will determine individual contributions to Eqs. (3)–(5) in an attempt to test the classical Turnbull description. To this extent we determine in chapter 3 and 4 interfacial tension and required contact angles. In chapter 5 we outline an independent measure of the surface free energy using the Laplace pressure, which can be compared to Turnbull predictions.

3 The Asakura-Oosawa model in the small polymer limit

If the ratio of polymer and colloid diameters $q = \sigma_p/\sigma_c$ is sufficiently small, $q < 0.154$, the equilibrium properties of the system can be exactly reduced to those of an equivalent one-component system, where the degrees of freedom of the polymers are integrated out, to yield an effective attractive potential among the colloids, given by (r is the distance between two colloid centres) [77]

$$U_{cc}(r)/k_BT = -\eta_p^r(1+1/q)^3\Big[1 - \frac{3r}{2\sigma_c(1+q)} + \frac{r^3}{2\sigma_c^3(1+q)^3}\Big], \quad \sigma_c < r < \sigma_c(1+q), \tag{6}$$

while $U_{cc}(r<\sigma_c) = \infty$ (overlap of hard spheres being forbidden) and $U_{cc}(r > \sigma_c(1+q)) = 0$. Here $\eta_p^r = (\pi\sigma_p^3/6)z_p$, z_p being the polymer fugacity, controls the strength of the attraction, and hence plays essentially the role of inverse temperature when one considers the phase diagram. While for $\eta_p^r = 0$ the model reduces to the simple hard sphere fluid, for which the colloid packing fractions $\eta = (\pi\sigma_c^3/6)\rho$ at liquid-solid phase coexistence are (see e.g. [78] and references therein) $\eta_f = 0.492$, $\eta_c = 0.545$, and the normalized pressure p_{coex} at phase coexistence is $p_{coex} = 11.576(6)\ k_BT/\sigma_c^3$. Of course, a meaningful study of nucleation is only possible when the properties of

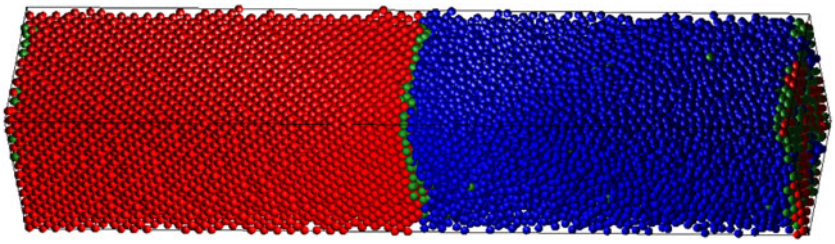

Fig. 1. Snapshot of a typical configuration of a crystal (red)/liquid (blue) slab for the interfacial velocity method. The lateral dimension is chosen as $L_x = L_y = L = na$, with a being the lattice constant and $L_z = 5L$ to avoid interactions between the interfaces (green) via periodic boundary conditions. Details can be found in [78].

the system at phase coexistence are very accurately known. For this purpose, the "interfacial velocity" method (see also [79] and references therein) was used: one studies an elongated system ($L \times L \times 5L$) with periodic boundary conditions throughout, where part of the system is a crystal and part the fluid, with two close-packed parallel $L \times L$ crystal-fluid interfaces. L is chosen such that the periodic boundary condition does not create any elastic distortion of the crystal at the considered pressure p, so L is commensurate with the crystal lattice. If $p < p_{coex}$, the volume fraction of the crystal shrinks (on average, considering a large number of Monte Carlo runs in the NpT ensemble); if $p > p_{coex}$, it grows (see [78,79] for computational details). Also the absence of significant size effects on p_{coex}, η_f, η_c for large enough L has been verified [78,79]. Choosing now (for $q = 0.15$) nonzero values of η_p^r, one observes a widening of the two-phase coexistence region with increasing η_p^r. For instance, for $\eta_p^r = 0.10$ phase coexistence occurs at $p_{coex} = 8.00 \pm 0.03\ k_BT/\sigma_c^3$ and $\eta_f \approx 0.494$, $\eta_c \approx 0.64$. While in the hard-sphere case numerous other studies exist in the literature (see [78,79] for references), and excellent agreement with the literature data was found, Ref. 78 gave the first application of this technique for the AO model. Recently, an extension of the approach to a "soft" variant of the AO model has been developed [80].

4 Estimation of wall excess free energies and surface tension

There exist numerous methods to study the wall excess free energies of fluid systems (see [23,81] for thorough comparisons of various of these methods), but most of them cannot be straightforwardly applied to wall excess free energies of a crystalline solid. Thus, a new approach has been developed (motivated by [82]), which is equally well suited for the estimation of wall excess free energies of both fluids and solids, the so-called "ensemble mixing method". One gradually transforms from a system without walls in the NVT ensemble, with periodic boundary conditions in all three space directions, to a system with two parallel walls at distance D from each other. For this system, periodic boundary conditions in the directions parallel to the walls are used. The volume is $V = L \times L \times D$ in both systems. One then constructs a system whose Hamiltonian is a mixture (at fractions $\kappa, 1-\kappa$) of both Hamiltonians $\mathcal{H}_1(\mathbf{X}), \mathcal{H}_2(\mathbf{X})$; note that both systems have the same configurational phase space points $\mathbf{X}$. Thus,

$$\mathcal{H}(\mathbf{X}) = (1-\kappa)\mathcal{H}_1(\mathbf{X}) + \kappa\mathcal{H}_2(\mathbf{X}), \quad \kappa \in [0,1]. \tag{7}$$

In practice, κ is discretized into a set of e.g. 100 discrete values $\{\kappa_i\}$, and, in addition to the standard Monte Carlo moves $\mathbf{X} \to \mathbf{X}'$, also moves where κ_i changes to a

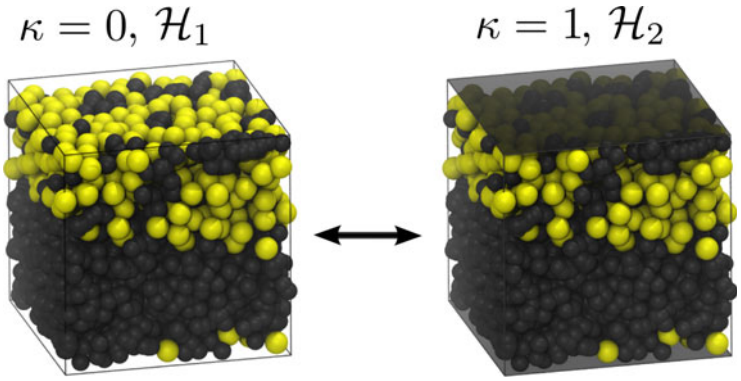

Fig. 2. Schematic description of the "ensemble mixing method". Periodic boundary conditions in x and y-direction are used and the simulation box is $L \times L \times D$ in size. κ denotes the mixture between the two Hamiltonians $\mathcal{H}_1$ and $\mathcal{H}_2$. In this case $\kappa = 0$ corresponds to a state with periodic boundary conditions in all directions, whereas $\kappa = 1$ corresponds to a state with walls in the z-plane. For further details see Deb et al. [81].

neighboring value κ_{i-1} or κ_{i+1} are considered and subjected the standard Metropolis test [83]. One samples the relative probability $P(i)$ to reside in state i, with a variant of Wang-Landau sampling [85] or successive umbrella sampling [84]. The free energy difference between the two states i and $i+1$ then follows from $k_BT[\ln P(i) - \ln P(i+1)]$. In this way the free energy difference $\Delta F(D)$ for any given choice D between a system with walls and without walls can be sampled. The wall excess free energy per unit area and k_BT then is

$$\gamma_{wf} = \lim_{D\to\infty} \Delta F(D)/(2L^2 k_B T). \tag{8}$$

Due to the excess density ρ_s at the walls, which in general is present at any systems with walls, so that $\rho = N/V = \rho_b + (2/D)\rho_s$, for any finite D the bulk density of the system with periodic boundary conditions (which is ρ by construction) will differ from the bulk density ρ_b in the system with walls slightly. Thus an extrapolation towards $D \to \infty$ is required (Fig. 3). This method works well also for the wall tension of the crystal, and hence the quantity $\Delta\gamma$ that enters Young's equation, Eq. (4), can be determined (Fig. 4).

Since already the estimation where the fluid-solid transition in the bulk is located has been based on studying the coexistence of fluid and solid domains separated by planar interfaces (Sect. 3), it is convenient to study the capillary waves that one expects to occur for rough interfaces [44] and extract an estimate of the interfacial stiffness $\tilde{\gamma}$ either from an analysis of the capillary wave spectrum [86–90] or the size-dependence of the interfacial width [78,79,86,89,91,92]. Note that the interfacial stiffness appears as energy parameter in the capillary wave Hamiltonian [44,93–95] that describes interfacial fluctuations

$$\mathcal{H}_{cw} = \frac{1}{2} k_B T \tilde{\gamma} \int_0^L dx \int_0^L dy [\nabla h(x,y)]^2 \tag{9}$$

where $h(x,y)$ is the height of the interface relative to its average position (which we define as the plane $z = 0$). By introducing Fourier transforms $h(\mathbf{q})$, where $\mathbf{q} = (q_x, q_y)$

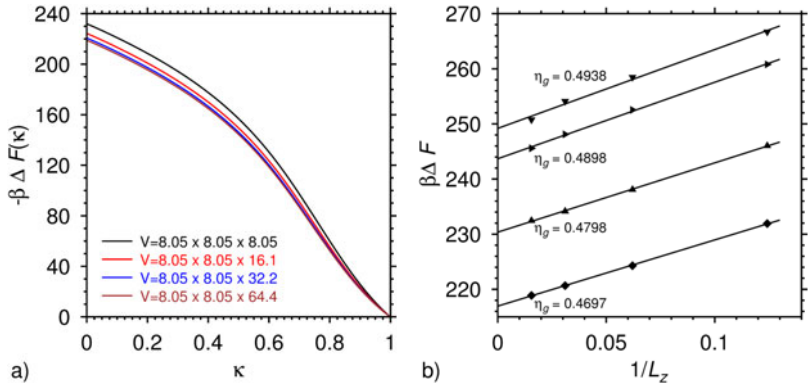

Fig. 3. Typical example that shows how wall tensions γ_{wf} are extracted using the ensemble mixing method for the AO model, using $q = 0.15$, $\eta_p^r = 0.1$, $L = 8.05\sigma_c$ and various choices of the wall distance L_z (here, $L_z \equiv D$). The wall potential is chosen as $U_{WCA}(z) = 4\varepsilon[(\sigma_w/z)^{12} - (\sigma_w/z)^6 + 1]$, $0 \le z \le \sigma_w 2^{1/6}$ and $\varepsilon/k_BT = 2.0$, $\sigma_w = \sigma_c/2$. Part (a) shows the total free energy difference $\Delta F(\kappa)/k_BT$ vs. κ for $\eta_b = 0.4697$. Part (b) shows the extrapolation to $1/D \to 0$ for several choices of η_b as indicated. The desired wall tension then is $\gamma_{wf} = \Delta F(0)\sigma_c^2/(2k_BTL^2)$. From Deb et al. [81].

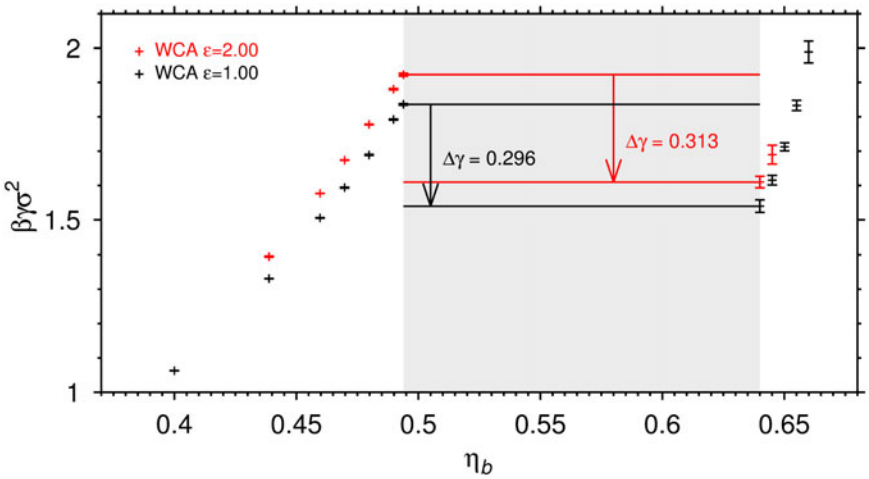

Fig. 4. Wall tensions of the AO model for $q = 0.15$, $\eta_p^r = 0.1$ and two choices of the wall potential mentioned in Fig. 3 ($\varepsilon/k_BT = 1$ or 2, respectively, as indicated) plotted vs. the bulk colloid packing fraction η_b. The difference $\Delta\gamma$ of the fluid and solid wall tensions at coexistence is indicated in both cases. The horizontal straight lines indicate the two-phase coexistence region. From Deb et al. [24].

is a two-dimensional wave vector in the plane $z = 0$, one can easily show that

$$\langle |h(\mathbf{q})|^2 \rangle = 1/(\tilde{\gamma} q^2) \tag{10}$$

and that the mean square interfacial width w^2 on a length scale L scales as

$$\langle w^2 \rangle = \text{const} + (4\tilde{\gamma})^{-1} \ln L \tag{11}$$

where the constant contains the (hypothetical! [91]) "intrinsic" interfacial width, and the small wavelength cutoff of the capillary wave spectrum for small enough

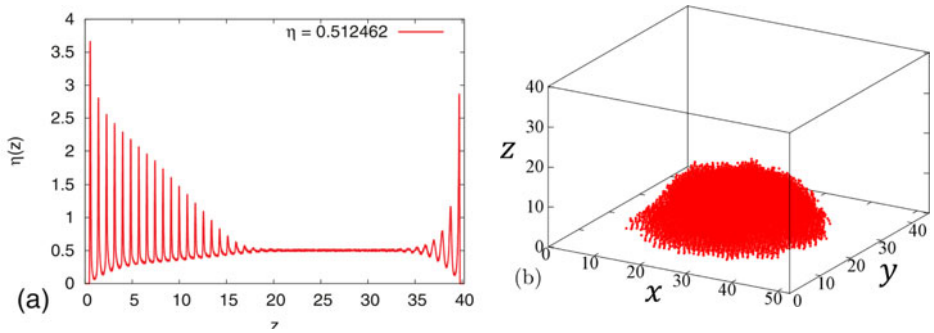

Fig. 5. a) Packing fraction profile $\eta(z)$ in the z-direction perpendicular to the walls at $z = 0$ and $z = D$, where $D = 40$. b) Snapshot picture of the crystalline droplet at packing fraction $\eta_c = 0.512462$. From Deb et al. [24].

q, Eq. (10), etc. We also note that for isotropic systems, where the interfacial tension does not depend on the interface orientation, we simply have $\tilde{\gamma} = \gamma$.

Now in systems for which γ can be extracted from sampling an "order parameter distribution", such as Ising models [97], symmetric polymer mixtures [86], or the gas-liquid-type transition in colloid-polymer mixtures [89], it has been shown that both Eqs. (10) and (11) can be used to obtain estimates for $\tilde{\gamma}$ with reasonable accuracy. Thus Zykova-Timan et al. [78] used Eq. (11) for the AO model to show that indeed also fluid-crystal interfaces exhibit capillary wave-induced broadening, and estimated $\sigma_c^2\tilde{\gamma} = (0.95 \pm 0.05)$ for the AO model discussed in Sect. 3. Together with the estimates for $\Delta\gamma$, one can then use Young's equation, Eq. (4), to obtain the estimate for the contact angle in this case, namely $\theta \approx 70^{\circ}$.

5 A Simulation of wall-attached crystalline droplets

In this section, we briefly review a simulation of the AO model of Sects. 3,4, in an $L \times L \times D$ geometry with two $L \times L$ walls a distance D apart, choosing again the same wall potential as in Fig. 3, with $\varepsilon = 1$, typical linear dimensions being $L = 39.6065\sigma_c$, $D = 40.3138\sigma_c$. Packing fractions η inside the two-phase coexistence region were chosen (e.g. $\eta = 0.512462$), and systems were simulated that did contain one "prefabricated" wall-attached crystalline "droplet", the volume of which was chosen according to the lever rule, using the known packing fractions η_f, η_c at fluid-crystal coexistence. Figure 5 shows that after suitable equilibration indeed wall-attached droplets of approximately sphere-cap shape are obtained. One can see that at the wall at $z = 0$ there is a well-developed layering of the packing fraction up to about $z = 17$, due to the presence of the crystalline droplet, while at the opposite wall there occurs only a rapidly decaying layering, typical for a fluid near a wall under partial wetting conditions. The distance between the peaks of $\eta(z)$ in the droplet reflects precisely the expected spacing, when one has a stacking of densely packed triangular crystal layers in the ABCABC... sequence, as appropriate for face-centered cubic (fcc) crystals.

In order to identify which particles belong to the crystalline nucleus in a particular configuration the Steinhardt order parameters [40–42] were used. They are defined in terms of the spherical harmonics $Y_{\ell m}$ as

$$q_{\ell m}(i) = \frac{1}{N(i)} \sum_{j=1}^{N(i)} Y_{\ell m}(\mathbf{r}_{ij}), \quad q_{\ell}(i) = \left(\frac{4\pi}{2\ell+1}\right) \sum_{m=-\ell}^{+\ell} |q_{\ell m}(i)|^2 \tag{12}$$

where $N(i)$ is the number of nearest neighbors of particle i, and $\mathbf{r}_{ij}$ the distance vector between i and j. Note that $\overline{q}_6(i)$ ($\overline{q}_6(i)$ refers to the averaged Steinhardt order parameter) in the fcc structure has a sharp peak at about $\overline{q}_6(i) \approx 0.56$, while $\overline{q}_\ell(i)$ in the fluid has a broad peak centered about $\overline{q}_6(i) \approx 0.15$. Of course, in the interfacial region the distribution of $\overline{q}_6(i)$ strongly broadens, and there is some inevitable arbitrariness which particles are still counted as belonging to the nucleus, or not. Nevertheless, it is gratifying that (in spite of large fluctuations) rather reasonable results for the average number of particles in the nucleus, the basal radius of the nucleus, the height H of the nucleus, and the contact angle θ were obtained, that were mutually compatible with each other in the framework of the assumption of a sphere cap nucleus shape, which in view of Fig. 5b seems reasonable. (From the number of particles in the fist crystalline layer adjacent to the basal plane N_b the radius $r = \sqrt{N_b/\rho_A \pi}$ is calculated. Here ρ_A is the areal density of the cluster base which is equal to $\rho_A = 4/\sqrt{3}(6\eta_m/4\pi)^{(2/3)}$. From the total number N^* of particles in the crystalline cluster one obtains the height H of the sphere cap via $N^* = \eta_m H(3r^2 + H^2)$. The contact angle follows as $\theta = \arccos[(r^2 - H^2)/(r^2 + H^2)]$, as stated in Deb et al. [24].) The result $\theta = (70 \pm 2)^\circ$ from this direct observation of the nucleus is in surprisingly good agreement with the prediction of the last section that was based on Young's equation.

Finally, we turn to a "thermodynamic" characterization of the nucleus, which does not need a "microscopic" identification of the particle configuration in the nucleus, but is based on an analysis of finite size effects in two-phase coexistence. This method has been used previously with good success to study nuclei in the lattice gas model [38,39], the Lennard-Jones model of fluids [63,65,67] and binary symmetric Lennard-Jones mixtures [66,98]. It is based on the fact that the interfaces associated with phase coexistence in finite systems cause non-negligible excess contributions to both the thermodynamic potential and its derivatives, and these excess terms contain useful information, from which interfacial free energies both of flat interfaces [97] and curved interfaces [38,39,63,65–67,98] can be extracted.

One consequence of these finite-size effects is that intensive variables such as the chemical potential μ or the pressure p, which in the thermodynamic limit must show a horizontal plateau throughout the two-phase coexistence region, rather exhibit a "loop" in finite systems. This "loop" has nothing whatsoever to do with van der Waals loops [99] (which would describe homogeneous phases rather than a two-phase region), and depends on the shape of the simulation box and on the boundary conditions. Figure 6 gives a schematic sketch of such a "loop" for the pressure for a (very large) $L \times L \times L$ system with periodic boundary conditions.

Using the techniques described by Deb et al. [23,81], the pressure in the fluid region surrounding the wall-attached droplet in Fig. 5 has actually been measured. For a droplet radius $R^* = 14.4\sigma$ a pressure enhancement $p' - p_{\mathrm{coex}} \approx 0.4 k_B T/\sigma^3$ was obtained. This result reflects the Laplace pressure effect [44]

$$p_c - p' = 2\gamma/R^* \tag{13}$$

where p_c is the pressure inside the crystalline nucleus. Since the chemical potential of the crystal and the surrounding fluid must be equal, we find from an expansion around the coexistence curve

$$\mu_c(p_c, T) = \mu_c(p_{\mathrm{coex}}, T) + v_c(p_c - p_{\mathrm{coex}}), \tag{14}$$

$$\mu_f(p', T) = \mu_f(p_{\mathrm{coex}}, T) + v_f(p' - p_{\mathrm{coex}}) \tag{15}$$

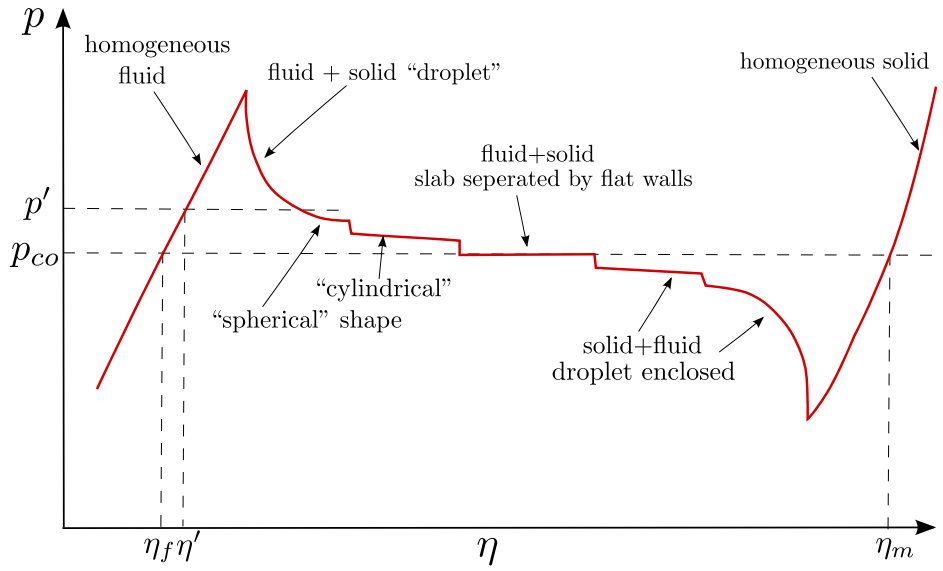

Fig. 6. Schematic description of the loop in the pressure versus packing fraction isotherm at a liquid to solid transition in a finite but very large simulation box. Note, however, that the transitions between the various regions shown are not sharp but rounded. At a pressure $p' > p_{co}$ we may have a homogeneous phase at $\eta' > \eta_f$ (which would be metastable for $L \to \infty$, but is stable for the chosen value of L), and in addition there occurs a state where a (spherical) solid "droplet" coexists with surrounding fluid having the same packing fraction η' and pressure p'. Adapted from Deb et al. [24].

where v_c, v_f are the volumes per particle taken in the coexisting crystal (c) and fluid (f) phases. So $p_c - p_{\rm coex} = (v_f/v_c)(p' - p_{\rm coex})$, and combining this result with Eq. (13) yields [100]

$$p_f - p_{\rm coex} = \frac{2\gamma}{R^*} \frac{\eta_f}{\eta_c - n_f} \approx 0.44 k_B T/\sigma^3. \tag{16}$$

Within the rather large errors of both the estimation of $p' - p_{\rm coex}$ and $\tilde{\gamma}$ (both quantities are known only within a relative statistical error of about 10%,), thus reasonable agreement is found.

Nevertheless, an immediate conclusion is that one needs to improve the accuracy of both estimations of θ, $\tilde{\gamma}$, and p' (and also a direct estimation of $\mu_f(p', T)$ would be desirable!) before one can proceed further; but this must be left to future work.

6 The need of going beyond the classical theory

Here we briefly discuss a few problems that have not yet been addressed for fluid-crystal nucleation, but have been found to be relevant for gas-liquid nucleation and or/nucleation in the lattice gas model.

(i) Curvature dependent surface tension $\gamma(R)$: already Tolman [50] has suggested that the surface tension of a spherical nucleus depends on its radius of curvature, and suggested that

$$\gamma(R) = \gamma(R = \infty)/\{1 + 2\delta/R + 2(\ell/R)^2\}, \quad R \to \infty, \tag{17}$$

where $\gamma(R=\infty)$ is a standard surface tension of planar interfaces, and the leading correction involves the "Tolman length" δ. Tolman [50] suggested that δ is of the order of a particle diameter, and positive for droplets; the subleading correction involves another length ℓ, and Tolman [50] assumed δ and ℓ to be of the same order. These suggestions have been controversial for many decades [51–68], but now an agreement is emerging that δ is much smaller than the molecular diameter, and negative for droplets (and hence positive for bubbles) [67]; only certain lattice models show a different behavior [68]. Since δ increases only weakly when the gas-liquid critical point is approached [61], actually the subleading term (since ℓ diverges at T_c proportional to the correlation length of density fluctuations) dominates in the critical region [66]. However, further work is needed to clarify the role of logarithmic corrections to Eq. (2) due to capillary wave fluctuations of the nucleus surface, translational entropy of the nucleus, etc. Note that sometimes a Tolman length depending on the droplet radius R is considered [67]; the Tolman length above is then understood as the limiting value for infinite radius.

(ii) Dependence of interfacial excess free energy $\gamma(\mathbf{n})$ on the orientation of the unit vector along the interface normal ($\mathbf{n}$) relative to a lattice direction: this problem could be rather relevant for fluid-crystal interfaces, and clearly is very relevant for the lattice gas model at low enough temperatures. E.g., in the latter case one can study [101] the gradual crossover of nucleus shape from a sphere to a cube (with rounded edges and corners at $T>0$) as the temperature is lowered. Since according to the classical theory the free energy barrier $\Delta F^*_{\rm hom}$ can be written for arbitrary nucleus shape as [101] $\Delta F^*_{\rm hom}=\frac{1}{2}(\rho_\ell-\rho_g)\Delta\mu V^*$, a simultaneous estimation of the nucleus volume (from the lever rule for the finite simulation box) and the chemical potential enhancement $\Delta\mu$ (using a lattice version of the Widom particle insertion method [102]) allows to study the enhancement of $\Delta F^*_{\rm hom}$ relative to the prediction of the classical theory that assumes a spherical shape [101]. While this enhancement is rather small when T clearly exceeds the roughening transition temperature T_R [103], for $T<T_R$ the enhancement rapidly rises for $T<T_R$ to reach its maximum value (for cubic nucleus shape) $6/\pi$ for $T=0$ [101]. This method to obtain $\Delta F^*_{\rm hom}$ relies on the principle that in equilibrium the chemical potential must be homogeneous throughout the system, irrespective of phase coexistence: thus, an actual determination of the crystal shape is not required. The latter task would require a complete knowledge of the angular dependence of $\gamma(\mathbf{n})$, so that the Wulff construction [71,104] can be carried out. It is defined by the set of points $W=\{x:\mathbf{x}\cdot\mathbf{n}\le\sigma(\mathbf{n})\}$ in the bulk and [72,73] $W=\{x:\mathbf{x}\cdot\mathbf{n}\le\tilde\sigma(\mathbf{n})\}$ for wall-attached crystals. Here $\tilde\sigma(\mathbf{n})=\Delta\sigma$ if $\mathbf{n}$ is oriented along the negative z direction and $\sigma(\mathbf{n})$ otherwise. However, it is not straightforward to carry out this construction in practice.

Another consequence of this anisotropy is a systematic distinction between interfacial free energy and interfacial stiffness. We discuss this point here only for interfaces that coincide with lattice planes, such as the plane $z=0$ in the simple cubic lattice model, and consider an interface tilted by a small angle ϑ relative to this interface, which then has an interfacial free energy $\gamma(\vartheta)$. For $T>T_R$ we have $\gamma(\vartheta)=\gamma(0)+\frac{1}{2}\kappa\vartheta^2$, and $\tilde\gamma(0)=\gamma+\kappa$ (see e.g. [105]).

Finally, we note that for such anisotropic interfaces Young's equation Eq. (4) for contact angle no longer holds, and gets replaced by [106]

$$\gamma(\theta)\cos\theta-\frac{d\gamma(\theta)}{d\theta}\sin\theta=\Delta\gamma. \tag{18}$$

(iii) Effects due to the line tension τ: an obvious generalization of Eq. (5) is [74–76]

$$\Delta F^*_{\rm het}=\Delta F^*_{\rm hom}f(\theta)+2\pi r\tau, \tag{19}$$

where r is the basal radius in the plane $z = 0$ of the wall attached droplet. For the lattice gas model at T distinctly larger than T_R, the numerical data of the simulations [38,39] seem to be compatible with Eq. (19), if for $\Delta F^*_{\rm hom}$ the curvature corrections in $\gamma(R)$ are included {Eq. (17)}. However, including both line tension and anisotropy effects together still remains to be done, even for the simple case of the lattice gas model.

7 Conclusion

In this mini-review, first steps to study heterogeneous nucleation barriers for wall-assisted heterogeneous nucleation of colloid crystals in colloid-polymer mixtures were described, in the framework of more general theoretical considerations. It was shown that the fluid-crystal interface in the Asakura-Oosawa model for colloid-polymer mixtures is rough, and hence planar interfaces exhibit capillary-wave induced broadening, while wall-attached crystalline nuclei do have approximately a sphere-cap shape, for conditions where the crystalline phase exhibits partial wetting of the planar wall. Therefore the classical Turnbull description {Eq. (4)} is a useful starting point, at least for very large nuclei it provides a first orientation. However, the accuracy with which crystal-fluid interfacial tensions and their dependence on interface orientation relative to the crystal axes can be determined still needs significant improvement, before a more systematic test of the theory is possible. For simpler models (lattice gases, gas-liquid transition of Lennard-Jones fluids, etc.) it has been found that effects due to the line tension and curvature corrections to the interface tension also matter, and are expected to play a role for the liquid-to-solid nucleation as well. It has been shown that some of these problems can be by-passed, via estimation of intensive variables (chemical potential, pressure) whose finite-size effects give direct information on the free energy barriers caused by the interfaces that need to be formed in heterogeneous nucleation events. Finally, also aspects of nucleation kinetics need to be addressed as well.

We thank J. Horbach, M. Oettel, R. Rozas, D. Wilms and M.H. Yamani for fruitful collaboration on some aspects of this work. This research was supported by The Deutsche Forschungsgemeinschaft in the framework of the SPP1296 (V1237/4-3). A. Tröster acknowledges support by the Austrian science fund (FWF) Project P22087-N16.

References

1. A.C. Zettlemoyer (ed.), *Nucleation* (M. Dekker, New York, 1969)
2. K. Binder, Rep. Progr. Phys. **50**, 783 (1987)
3. D. Kashchiev, *Nucleation: Basic Theory with Applications* (Butterworth-Heinemann, Oxford 2000)
4. S. Dietrich, *Phase Transitions and Critical Phenomena*, Vol. XII, edited by C. Domb, L. Lebowitz (Academic Press, London 1988), p. 1
5. D. Bonn, J. Eggers, J. Indekeu, J. Meunier, E. Ratley, Rev. Mod. Phys. **81**, 939 (2009)
6. J. Hernandez-Guzman, E.R. Weeks, PNAS **106**, 15198 (2009)
7. H. Löwen, J. Phys.: Condens. Matter **13**, R415 (2001)
8. H.N.W. Lekkerkerker, W.C.K. Poon, P.N. Pusey, A. Stroebants, R. Warren, Europhys. Lett. **20**, 559 (1992)
9. S.M. Ilett, A. Orrock, W.C.K. Poon, P.N. Pusey, Phys. Rev. E **51**, 344 (1995)
10. W.C.K. Poon, J. Phys.: Condens. Matter **14**, R 859 (2002)

11. S. Asakura, F. Oosawa, J. Chem. Phys. **22**, 1255 (1954)
12. S. Asakura, F. Oosawa, J. Polym. Sci.: Polymer Phys. Ed. **23**, 183 (1958)
13. A. Vrij, Pure Appl. Chem. **48**, 471 (1976)
14. J. Zausch, P. Virnau, K. Binder, J. Horbach, R.L.C. Vink, J. Chem. Phys. **130**, 064906 (2009)
15. P.G. de Gennes, *Scaling Concepts in Polymer Physics* (Correll Univ. Press, Ithaca, 1979)
16. S. Auer, D. Frenkel, Nature **409**, 1020 (2001)
17. L. Filion, R. Ni, D. Frenkel, M. Dijkstra, J. Chem. Phys. **134**, 134901 (2011)
18. T. Schilling, S. Dorosz, H.J. Schöpe, G. Opletal, J. Phys.: Condens. Matter **25**, 194129 (2011)
19. S. Auer, D. Frenkel, Phys. Rev. Lett. **91**, 015703 (2003)
20. A. Cacciuto, S. Auer, D. Frenkel, Nature **428**, 404 (2004)
21. A. Cacciuto, D. Frenkel, Phys. Rev. E **72**, 041604 (2005)
22. M. Dijkstra, Phys. Rev. Lett. **93**, 108303 (2004)
23. D. Deb, A. Winkler, M.H. Yamani, M. Oettel, P. Virnau, K. Binder, J. Chem. Phys. **134**, 214706 (2011)
24. D. Deb, A. Winkler, P. Virnau, K. Binder, J. Chem. Phys. **136**, 134710 (2012)
25. A. Statt, A. Winkler, P. Virnau, K. Binder, J. Phys.: Condens. Matter **24**, 464122 (2012)
26. A. Winkler, A. Statt, P. Virnau, K. Binder, Phys. Rev. E **87**, 03207 (2013)
27. K. Binder, J. Horbach, R.L.C. Vink, A. De Virgiliis, Soft Matter **4**, 1555 (2008)
28. R.C. Advincula, W.J. Brittain, K.C. Castler, J. Rühe (eds.), *Polymer Brushes* (Wiley-VCH, Weinheim, 2004)
29. K. Binder, A. Milchev, J. Polymer Sci., Ser. B, Polymer Phys. **50**, 1515 (2012)
30. D.M. Napper, *Polymeric Stabilization of Colloidal Disperions* (Academic Press, London 1983)
31. K. Schätzel, B.J. Ackerson, Phys. Rev. E **48**, 3766 (1993)
32. J.L. Harland, W. van Megen, Phys. Rev. E **55**, 8054 (1997)
33. S. Iacopini, T. Palberg, H.-J. Schöpe, J. Chem. Phys. **130**, 084502 (2009)
34. D. Turnbull, J. Appl. Phys. **21**, 1022 (1950)
35. D. Turnbull, J. Chem. Phys. **18**, 198 (1950)
36. J.E. Burke, D. Turnbull, Progr. Met. Phys. **3**, 220 (1952)
37. H. Biloni, in R.W. Cahn, P. Haasen (eds.), *Physical Metallurgy* (North-Holland, Amsterdam, 1983), p. 477
38. D. Winter, P. Virnau, K. Binder, Phys. Rev. Lett. **103**, 225703 (2009)
39. D. Winter, P. Virnau, K. Binder, J. Phys.: Condens. Matter **21**, 464118 (2009)
40. P.J. Steinhardt, D.R. Nelson, M. Ronchetti, Phys. Rev. B **28**, 783 (1983)
41. P.R. ten Wolde, M.J. Ruiz-Montero, D. Frenkel, Phys. Rev. Lett. **75**, 2414 (1995)
42. W. Lechner, C. Dellago, J. Chem. Phys. **129**, 114707 (2008)
43. J.W. Gibbs, *The Collected Works of J. Willard Gibbs* (Yale Univ. Press. London, 1957), p. 288
44. J.S. Rowlinson, B. Widom, *Molecular Theory of Capillarity* (Clarendon Press, Oxford, 1982)
45. J.O. Indekeu, Int. J. Mod. Phys. B **38**, 309 (1994)
46. J. Drelich, Colloids Surf. A **116**, 43 (1995)
47. T. Getta, S. Dietrich, Phys. Rev. E **57**, 655 (1998)
48. C. Bauer, S. Dietrich, Eur. Phys. J. B **10**, 767 (1999)
49. K. Binder, D, Stauffer, Adv. Phys. **25**, 343 (1976)
50. R.C. Tolman, J. Chem. Phys. **17**, 333 (1949)
51. M.P.A. Fisher, M. Wortis, Phys. Rev. B **29**, 6252 (1984)
52. S.M. Thompson, K.E. Gubbins, J.P.R.B. Walton, R.A.R. Chamry, J.S. Rowlinson, J. Chem. Phys. **81**, 530 (1984)
53. M.J.P. Nijmeijer, C. Bruin, A.B. van Woeshom, A.F. Bakker, J. Chem. Phys. **96**, 595 (1992)

54. E.M. Blokhuis, D. Bedeaux, Physica A **184**, 42 (1992)
55. E.M. Blokhuis, D. Bedeaux, J. Chem. Phys. **97**, 3976 (1992)
56. J.M. Rowlinson, J. Phys.: Condens. Matter **6**, A1 (1994)
57. V. Tabanquer, D.W. Oxtoby, J. Phys. Chem. **99**, 2865 (1995)
58. L. Granasy, J. Chem. Phys. **109**, 9660 (1998)
59. A.E. van Giessen, E.M. Blokhuis, D.J. Bukman, J. Chem. Phys. **108**, 1148 (1998)
60. P.R. ten Wolde, D. Frenkel, J. Chem. Phys. **109**, 9901 (1998)
61. M.A. Anisimov, Phys. Rev. Lett. **98**, 035702 (2007)
62. A.E. van Giessen, E.M. Blokhuis, J. Chem. Phys. **131**, 164705 (2009)
63. M. Schrader, P. Virnau, K. Binder, Phys. Rev. E **79**, 061104 (2009)
64. J.G. Sampayo, A. Malijevsky, E.A. Müller, E. de Miguel, G. Jackson, J. Chem. Phys. **132**, 141101 (2010)
65. B.J. Block, S.K. Das, M. Oettel, P. Virnau, K. Binder, J. Chem. **133**, 154702 (2010)
66. S.K. Das, K. Binder, Phys. Rev. Lett. **107**, 235702 (2011)
67. A. Tröster, M. Oettel, B.J. Block, P. Virnau, K. Binder, J. Chem. Phys. **136**, 064709 (2012)
68. A. Tröster, K. Binder, Phys. Rev. Lett. **107**, 265701 (2011)
69. T. Schilling, S. Dorosz, M. Radu, M. Mathew, S. Jungblut, K. Binder, Eur. Phys. J. Special Topics (2013) (in press)
70. M. Radu, T, Schilling [`arXiv.1301.5592`] [cond-mat-soft] (2013)
71. G. Wulff, Z. Kristallogr, Mineralogie **34**, 449 (1901)
72. W.L. Winterbottom, Act. Metall. **15**, 303 (1967)
73. J. Ill. Avron, J.E. Taylor, R.K.P. Zia, J. Stat. Phys. **33**, 493 (1983)
74. R.D. Gretz, J. Chem. Phys. **45**, 3160 (1966)
75. G. Nawascues, P. Taranzona, J. Chem. Phys. **75**, 2441 (1981)
76. P.S. Swain, R. Lipowsky, Langmuir **14**, 6772 (1998)
77. M. Dijkstra, R. van Roij, R. Evans, Phys. Rev. E **59**, 5744 (1999)
78. T. Zykova-Timan, J. Horbach, K. Binder, J. Chem. Phys. **133**, 014705 (2010)
79. T. Zykova-Timan, R.E. Rozas, J. Horbach, K. Binder, J. Phys.: Condens. Matter **21**, 464102 (2009)
80. A. Statt, P. Virnau, K. Binder (unpublished)
81. D. Deb, D. Wilms, A. Winkler, P. Virnau, K. Binder, Int. J. Mod. Phys. C **23**, 124001 (2012)
82. M. Heni, H. Löwen, Phys. Rev. E **60**, 7057 (1999)
83. K. Binder, Rep. Progr. Phys. **60**, 487 (1997)
84. P. Virnau, M. Müller, J. Chem. Phys. **120**, 10925 (2004)
85. F. Wang, D.P. Landau, Phys. Rev. Lett. **86**, 2050 (2001)
86. A. Werner, F. Schmid, M. Müller, K. Binder, Phys. Rev. E **59**, 728 (1999)
87. J.J. Hoyt, M. Asta, A. Karma, Phys. Rev. Lett. **86**, 5530 (2001)
88. M. Asta, J.J. Hoyt, A. Karma, Phys. Rev. B **66**, 100101 (R) (2002)
89. R.L.C. Vink, J. Horbach, K. Binder, J. Chem. Phys. **122**, 134905 (2005)
90. R.E. Rozas, J. Horbach, EPL **93**, 26006 (2011)
91. K. Binder, M. Müller, Inst. J. Mod. Phys. C **11**, 1093 (2000)
92. S. Wolfheimer, C. Tanase, K. Shundyak, R. van Roij, T. Schilling, Phys. Rev. E **73**, 061703 (2006)
93. F.P. Buff, R.A. Lovett, F. Stillinger, Phys. Rev. Lett. **15**, 621 (1965)
94. B. Widom, *Phase Transitions and Critical Phenomena*, Vol. 2, edited by C. Domb, M.S. Green (Academic Press, London, 1972), p. 79
95. J.D. Weeks, J. Chem. Phys. **67**, 3106 (1977)
96. D. Jasnow, Rep. Progr. Phys. **47**, 1059 (1984)
97. K. Binder, Phys. Rev. A **25**, 1699 (1982)
98. S.K. Das, K. Binder, Mol. Phys. **109**, 1043 (2011)
99. K. Binder, B.J. Block, P. Virnau, A. Tröster, Am. J. Phys. **80**, 1099 (2012)
100. Note that Eq. (17) of [24] and the subsequent claim of a significant discrepancy is an error

101. F. Schmitz, P. Virnau, K. Binder, Phys. Rev. E **87**, 053302 (2013)
102. B. Widom, J. Phys. Chem. **86**, 869 (1982)
103. J.D. Weeks, *Ordering in Strongly Fluctuating Condensed Matter Systems*, edited by T. Riste (Plenum Press, New York, 1980), p. 293
104. C. Herring, Phys. Rev. **82**, 87 (1951)
105. V.P. Privman, Int. J. Mod. Phys. C **3**, 857 (1992)
106. R.K.P. Zia, *Statistical and Particle Physics. Common Problems and Techniques*, edited by K.C. Bowler, A.J. McKane (Scottish Univ. Press, Edinburgh, 1984), p. 247